Phyllotaxis and patterns on plants

Alan C. Newell, Zhiying Sun, Patrick D. Shipman

University of Arizona

March 23, 2009

THE UNIVERSITY OF ARIZONA

Patterns Are Everywhere

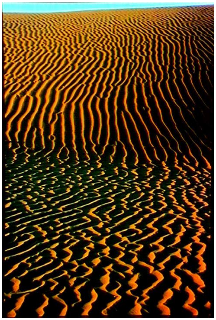

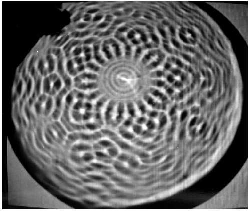

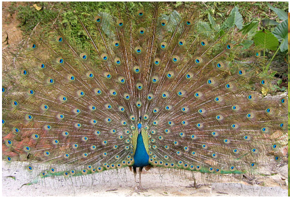

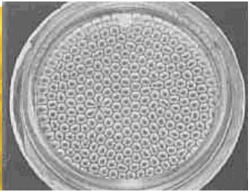

More Examples of Patterns on Plants

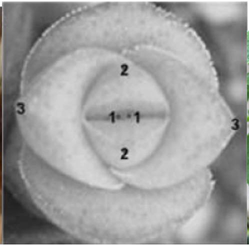

THE UNIVERSITY OF ARIZONA

More Examples of Patterns on Plants

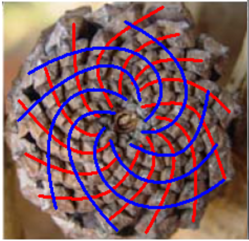

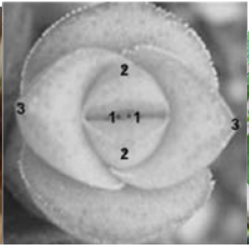

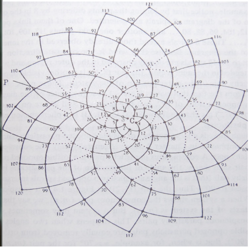

How does leaves/flowers form on a plant?

Mature
sunflower head

Apical meristem(AM)

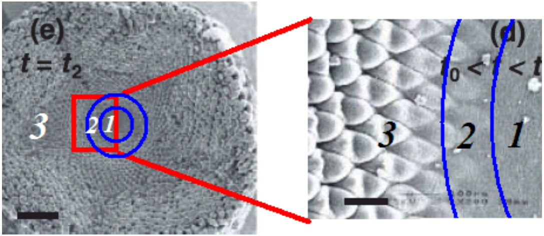

Schematic of AM

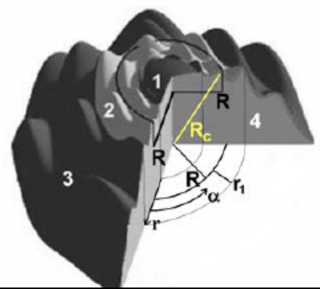

Diagrams of phylla formation

Circular View

$t = t_1$

Rectangular View

Movement of the Controlling parameter

Diagrams of phylla formation

Circular View

Rectangular View

Movement of the Controlling parameter

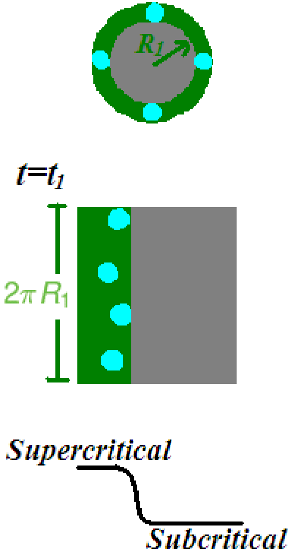

Diagrams of phylla formation

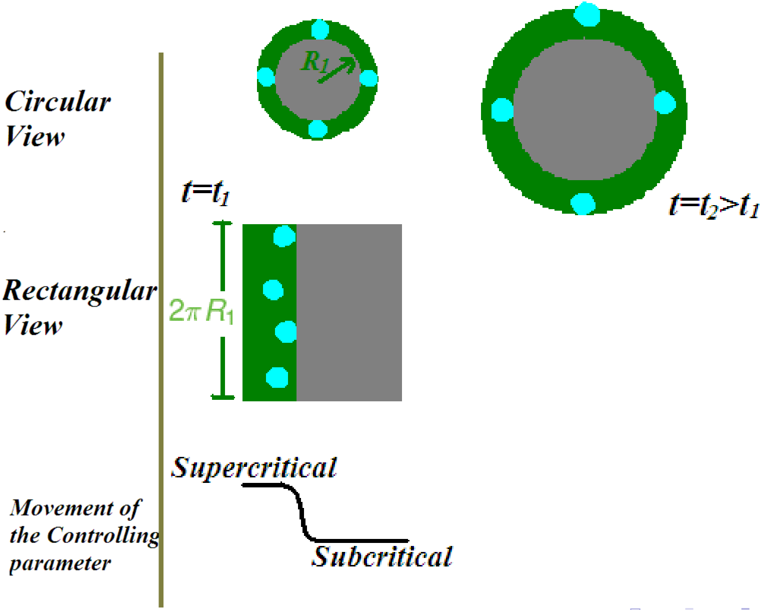

Diagrams of phylla formation

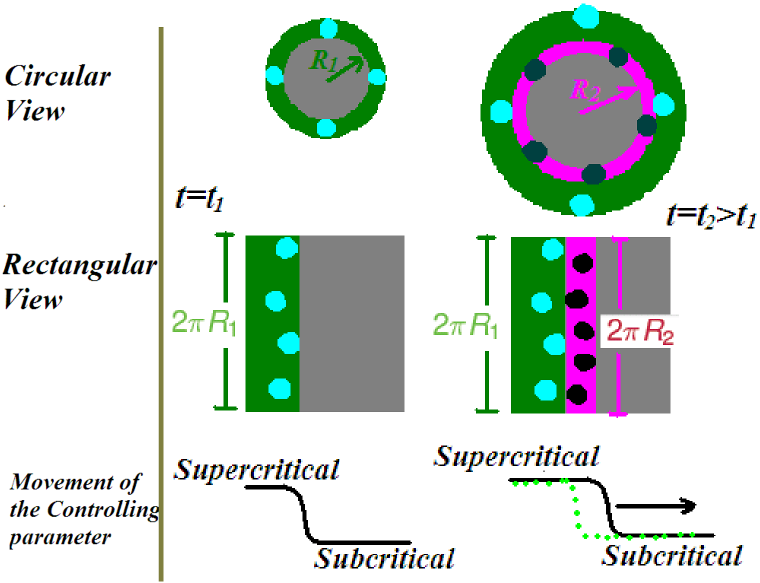

Plant patterns

Challenges:

- Why Fibonacci?
- Connection between phyllotactic configurations and surface deformations
- Transitions
- Universality, self similarity
- Are plant patterns seen anywhere else in the physical world or the laboratory?

Mechanisms and models

Paradigms:	Hofmeister (1868), Snow and Snow(1950's) Douady and Couder (1990's)
Mechanical stresses:	Green, Steele, Dumais (1990's) Shipman and Newell (2005)
Biochemical agents:	Reinhardt et al (2000) Meyerowitz et al (2007) Traas et al (2007)
Coupled model:	Growth affects stress/strain Stress promotes growth.

How do we connect paradigms and mechanisms?

Paradigms and Mechanisms: connections?

Paradigms are rules for the placement of the newest primordium given the positions of all previous primordia.

cf. packing efficiency

Mechanisms involve instabilities of uniform states, the decomposition of the phase space into active A and passive P(A) modes, the coordinatization of A with (amplitude) order parameters, and order parameter equations which may be gradient flows with a free energy.

cf. energy minimization

How to connect these ideas?

Biochemical factors

- Reinhardt (2000) showed that hormone Auxin is instrumental in growth and uneven distribution of Auxin is the reason for the formation of phyllotaxis

THE UNIVERSITY OF ARIZONA.

Biochemical factors

- Reinhardt (2000) showed that hormone Auxin is instrumental in growth and uneven distribution of Auxin is the reason for the formation of phyllotaxis
- Meyerowitz, Traas, Reinhardt et al (2006): Auxin efflux protein PIN1 on the cell wall can redistribute themselves so as to pump Auxin form low concentration to high concentration

$$\frac{dA(i)}{dt} = D\sum_k (A(k) - A(i)) + T\sum_k (A(k)P(k,i) - A(i)P(i,k)) + c - dA(i)$$

$$P(i,j) = P_{ij} = P\frac{A(j)}{\kappa + \sum_j^{(k)} A(k)}$$

$A(i)$: Auxin concentration in cell i
$P(i,k)$: PIN1 concentration on cell wall (i,j) pointing to cell j

Biochemical factors

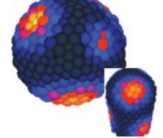

- Reinhardt (2000) showed that hormone Auxin i... in growth and uneven distribution of Auxin is the r... formation of phyllotaxis
- Meyerowitz, Traas, Reinhardt et al (2006): Auxin efflux protein PIN1 on the cell wall can redistribute themselves so as to pump Auxin form low concentration to high concentration

$$\frac{dA(i)}{dt} = D\sum_k (A(k) - A(i)) + T\sum_k (A(k)P(k,i) - A(i)P(i,k)) + c - dA(i)$$

$$P(i,j) = P_{ij} = P\frac{A(j)}{\kappa + \sum_j^{(k)} A(k)}$$

$A(i)$: Auxin concentration in cell i

$P(i,k)$: PIN1 concentration on cell wall (i,j) pointing to cell j

The continuum limit PDE:

$$g_t = -Lg - H\nabla^2 g - \nabla^4 g - \bar{\kappa}_1 \nabla(g\nabla g) - \bar{\kappa}_2 \nabla(\nabla g \nabla^2 g) - \delta' g^3$$

$g(r,\alpha)$: auxin fluctuation around stationary uniform concentration $\sim$ growth strain

Mechanical Factors

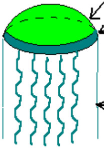

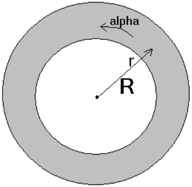

FvKD Equation(Describing deformation of thin elastic shells):

$$\zeta w_t + D\Delta^2 w + N\Delta_\chi w + \frac{1}{R_\alpha}\Delta_\rho f - [f, w] + \kappa w + \gamma w^3 = 0$$

$$\frac{1}{Eh}\Delta^2 f - \frac{1}{R_\alpha}\Delta_\rho w + \frac{1}{2}[w, w] = 0$$

$w(r, \alpha)$: out-of-surface deformation. $f(r, \alpha)$: in-plane stress.

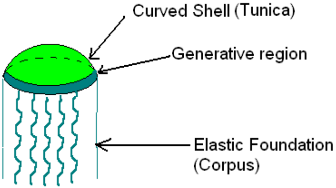

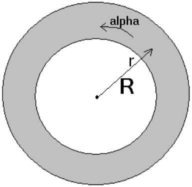

FvKD Equation(Describing deformation of thin elastic shells):

$$\zeta w_t + D\Delta^2 w + N\Delta_\chi w + \frac{1}{R_\alpha}\Delta_\rho f - [f, w] + \kappa w + \gamma w^3 = 0$$

$$\frac{1}{Eh}\Delta^2 f - \frac{1}{R_\alpha}\Delta_\rho w + \frac{1}{2}[w, w] = 0$$

$w(r, \alpha)$: out-of-surface deformation. $f(r, \alpha)$: in-plane stress.

Combined Model

Equations for coupled model

$w(r, \alpha, t)$ Surface normal deformation
$f(r, \alpha, t)$ Airy Stress tensor
$g(r, \alpha, t)$ Growth/fluctuation auxin concentration

$$\zeta w_t + D\Delta^2 w + N\Delta_\chi w + \frac{1}{R_\alpha}\Delta_\rho f - [f, w] + \kappa w + \gamma w^3 = 0$$
$$\frac{1}{Eh}\Delta^2 f - \frac{1}{R_\alpha}\Delta_\rho w + \frac{1}{2}[w, w] + \Delta g = 0$$
$$g_t = -Lg - H \bigtriangledown^2 g - \bigtriangledown^4 g - \bar{\kappa}_1 \bigtriangledown (g \bigtriangledown g) - \bar{\kappa}_2 \bigtriangledown (\bigtriangledown g \bigtriangledown^2 g) - \delta g^3 + \beta \Delta f$$

Patterns arising from the governing equations

Both mechanisms share the same structures in the equations.
$\frac{\partial w}{\partial t} = -(\nabla^2 + P)^2 w + \epsilon w + N.L.$.
In 1-dimensional, The linear growth rate for $e^{ikx+\sigma t}$ is
$\sigma(k) = (-k^2 + P)^2 + \epsilon$.
In 2-dimensional, $\nabla^2 = \frac{\partial^2}{\partial r^2} + \frac{1}{r}\frac{\partial}{\partial r} + \frac{1}{r^2}\frac{\partial^2}{\partial \alpha^2}$ The linear growth rate for $e^{il\alpha + imx + \sigma t}$ is $\sigma(l, m) = -(-l^2 - \frac{m^2}{r^2} + P)^2 + \epsilon$.

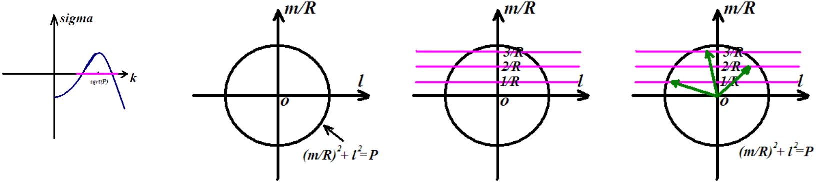

Triad: $\vec{k}_m = (l_m, m), \vec{k}_m + \vec{k}_n = \vec{k}_{m+n} \Rightarrow l_m + l_n = l_{m+n}, m + n = (m + n)$

Amplitude Equations 1. Representation

$$w(r,\alpha,t) = \sum A_m^s(r,t)e^{is\int l_m dr - im\alpha} + (*)$$

where $A_m(r,t)e^{i\int l_m dr}$ is WKB approximation for Hankel functions $H_m^s(kr)$ in the $r >> 1$, m/r finite limit with $l_m^2 = k^2 - m^2/r^2$

$$g(r,\alpha,t) = \sum B_m^s(r,t)e^{is\int l_m dr - im\alpha} + (*)$$

Linear

$$\frac{\partial A_m}{\partial t} + (2il_m\frac{\partial}{\partial r} + i\frac{\partial l_m}{\partial r} + i\frac{l_m}{r})^2 A_m = (\epsilon - (l_m^2 + \frac{m^2}{r^2} - P)^2)A_m$$

Quadratic nonlinearity

$$e^{i\int l_m dr - im\alpha} e^{i\int l_n dr - in\alpha} \longrightarrow e^{i\int (l_m+l_n)dr - i(m+n)\alpha}$$

$$+\tau(m, n, m+n)A_n^* A_{m+n}$$

Cubic Saturation (e.g. elastic foundation response)

$$-\gamma A_m(|A_m|^2 + \sum \delta_{ms}|A_s|^2)$$

Energy Functional

$$
\begin{aligned}
E\{A_m, A_m*, ...\} = \quad & - \quad \sum \sigma_m A_m A_m^* \\
& - \quad \sum \tau_{jpq}(A_j^* A_p A_q + (*)) \\
& + \quad \gamma \sum (\frac{1}{2}|A_m|^4 + \sum_{m \neq s} \delta_{ms}|A_m|^2|A_s|^2)
\end{aligned}
$$

Adiabatic response

- Solve stationary amplitude equations

$$A_j(l_m, l_n, r)$$

- Choose l_m, l_n to minimize E

Outcome

Theorem: The amplitude equations for ANY Fibonacci sequence are invariant under $R \to R\phi$, $\phi = \frac{\sqrt{5}+1}{2}$, the golden number;

$$A_j^s(R) \to A_{j+1}^{-s}(R\phi), \quad l_j(R) \to -l_{j+1}(R\phi), \quad m_j \to m_{j+1}(\simeq m_j\phi)$$

1,2,3,5,8,13,...

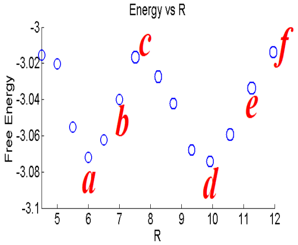

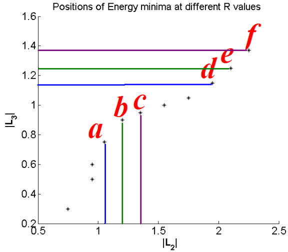

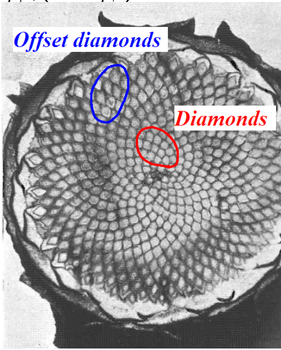

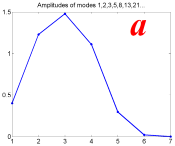

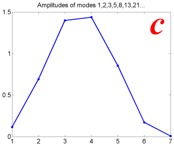

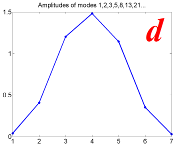

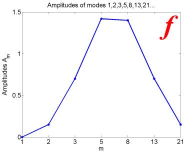

PDE Simulation

$$r = r_0 + Ut - r' \qquad \nabla^2 = \frac{1}{R}\frac{\partial}{\partial r'} R \frac{\partial}{\partial r'} + \frac{1}{R^2}\frac{\partial^2}{\partial \alpha^2} \qquad R = r_0 + (\frac{U}{V} - 1)r'$$

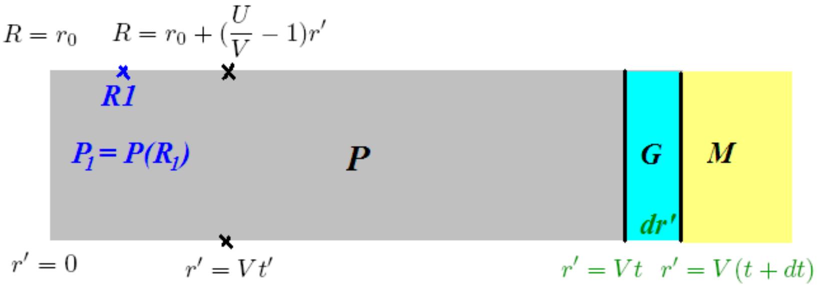

PDE Simulation

Front propagating outwards (radius increasing $R \in [2, 7]$, $\alpha \in [0, 2\pi]$)

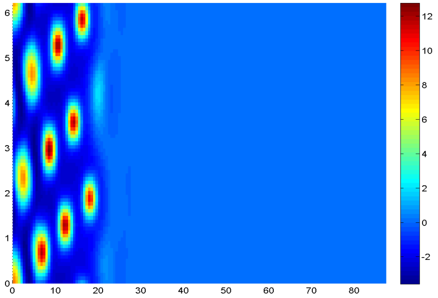

Fourier Space:
(Frequency)

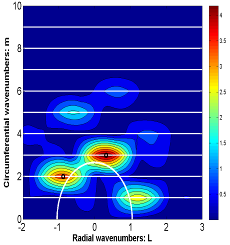

Front propagating outwards (radius increasing $R \in [2, 7]$, $\alpha \in [0, 2\pi]$)

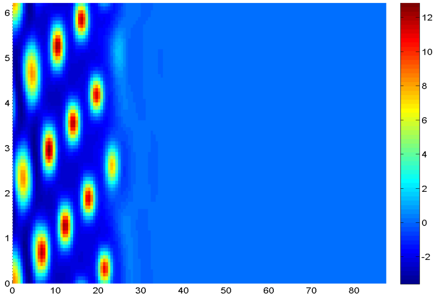

Fourier Space:
(Frequency)

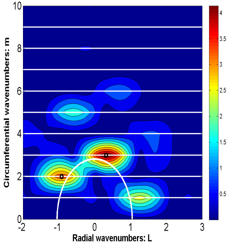

Front propagating outwards (radius increasing $R \in [2, 7]$, $\alpha \in [0, 2\pi]$)

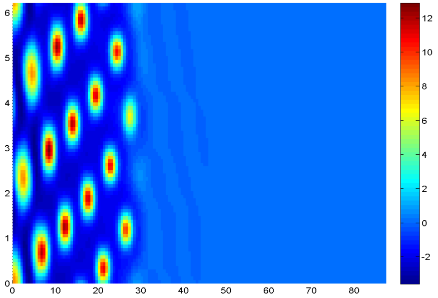

Fourier Space:
(Frequency)

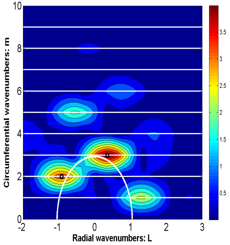

PDE Simulation

Front propagating outwards (radius increasing $R \in [2, 7]$, $\alpha \in [0, 2\pi]$)

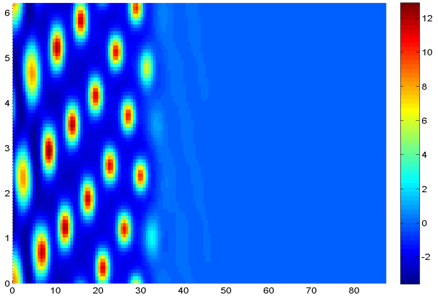

Fourier Space: (Frequency)

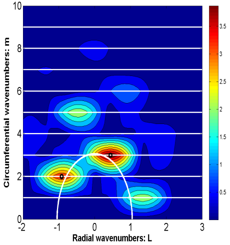

PDE Simulation

Front propagating outwards (radius increasing $R \in [2, 7]$, $\alpha \in [0, 2\pi]$)

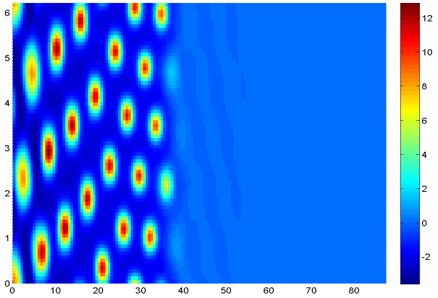

Fourier Space: (Frequency)

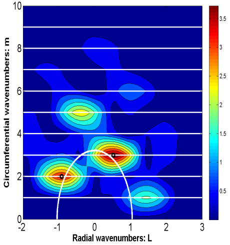

PDE Simulation

Front propagating outwards (radius increasing $R \in [2, 7]$, $\alpha \in [0, 2\pi]$)

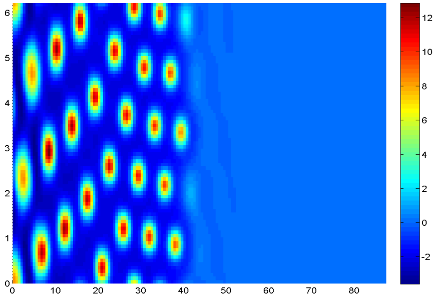

Fourier Space:
(Frequency)

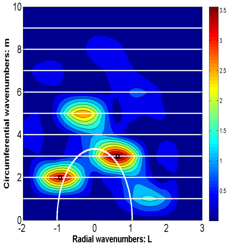

PDE Simulation

Front propagating outwards (radius increasing $R \in [2, 7]$, $\alpha \in [0, 2\pi]$)

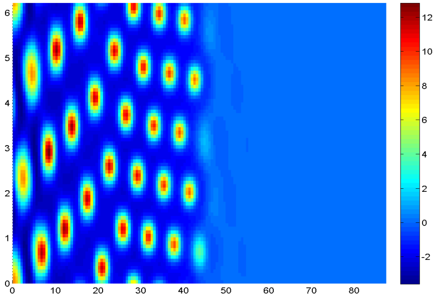

Fourier Space:
(Frequency)

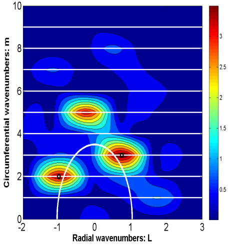

PDE Simulation

Front propagating outwards (radius increasing $R \in [2, 7]$, $\alpha \in [0, 2\pi]$)

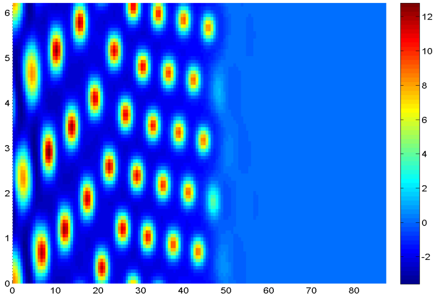

Fourier Space: (Frequency)

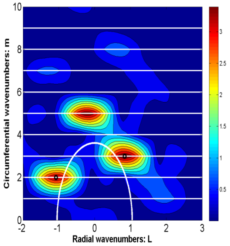

Front propagating outwards (radius increasing $R \in [2, 7]$, $\alpha \in [0, 2\pi]$)

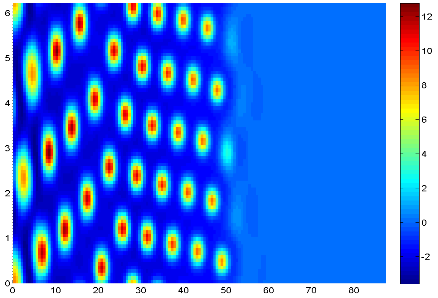

Fourier Space:
(Frequency)

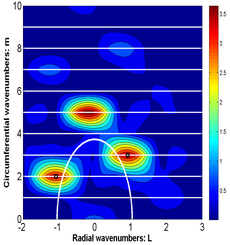

Front propagating outwards (radius increasing $R \in [2, 7]$, $\alpha \in [0, 2\pi]$)

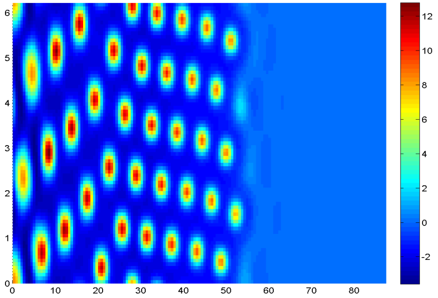

Fourier Space: (Frequency)

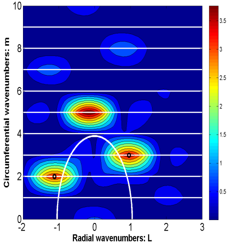

Front propagating outwards (radius increasing $R \in [2, 7]$, $\alpha \in [0, 2\pi]$)

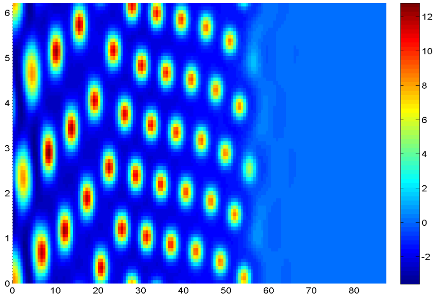

Fourier Space:
(Frequency)

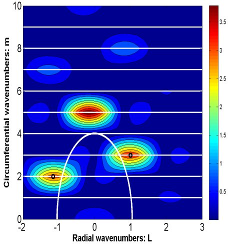

THE UNIVERSITY OF ARIZONA

Front propagating outwards (radius increasing $R \in [2,7]$, $\alpha \in [0, 2\pi]$)

Fourier Space:
(Frequency)

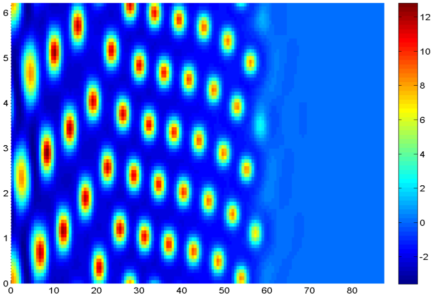

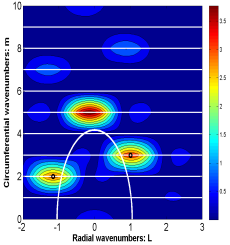

Front propagating outwards (radius increasing $R \in [2, 7]$, $\alpha \in [0, 2\pi]$)

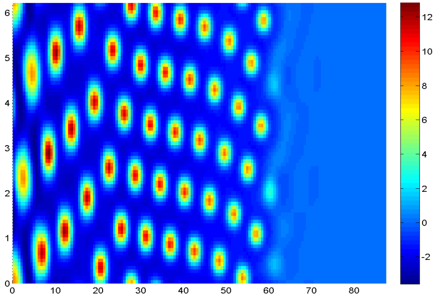

Fourier Space:
(Frequency)

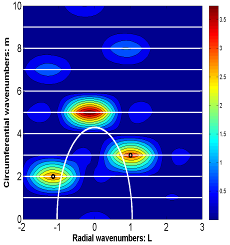

PDE Simulation

Front propagating outwards (radius increasing $R \in [2, 7]$, $\alpha \in [0, 2\pi]$)

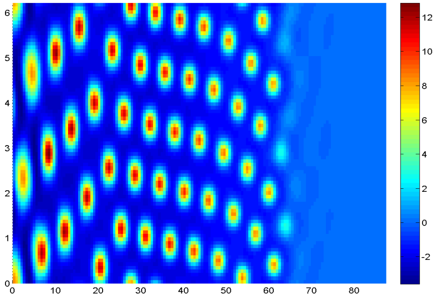

Fourier Space: (Frequency)

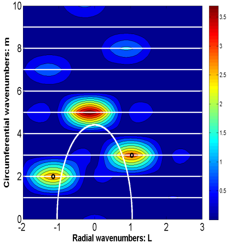

PDE Simulation

Front propagating outwards (radius increasing $R \in [2, 7]$, $\alpha \in [0, 2\pi]$)

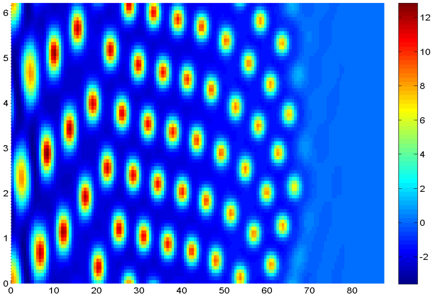

Fourier Space:
(Frequency)

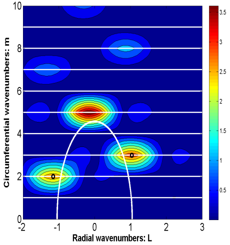

PDE Simulation

Front propagating outwards (radius increasing $R \in [2, 7]$, $\alpha \in [0, 2\pi]$)

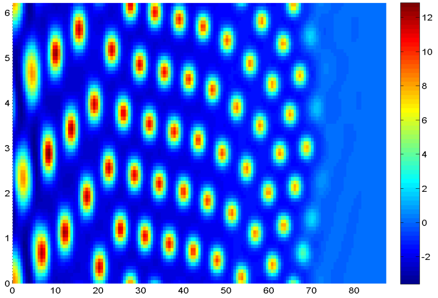

Fourier Space:
(Frequency)

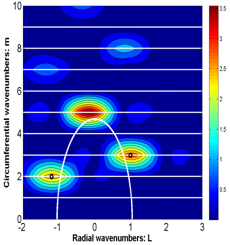

Front propagating outwards (radius increasing $R \in [2, 7]$, $\alpha \in [0, 2\pi]$)

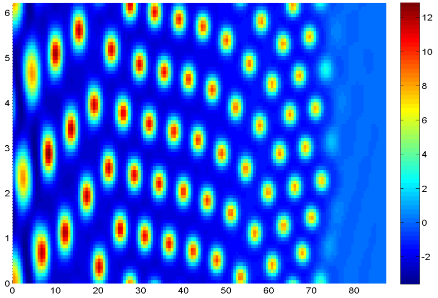

Fourier Space: (Frequency)

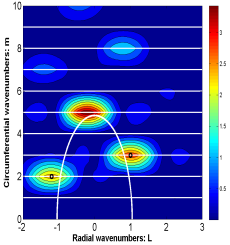

PDE Simulation

Front propagating outwards (radius increasing $R \in [2,7]$, $\alpha \in [0, 2\pi]$)

Fourier Space:
(Frequency)

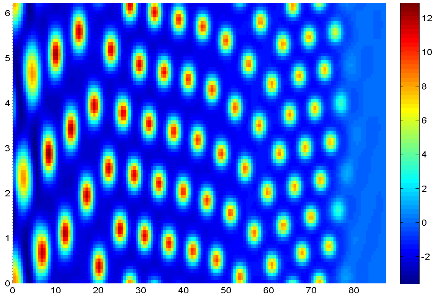

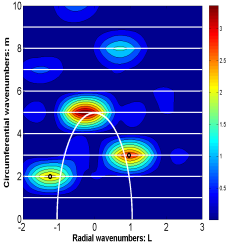

Front propagating outwards (radius increasing $R \in [2, 7]$, $\alpha \in [0, 2\pi]$)

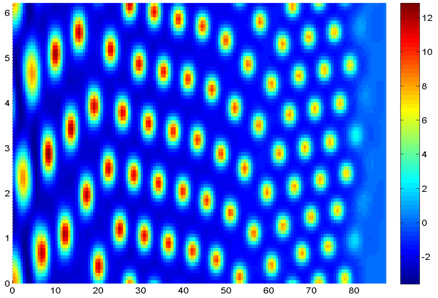

Fourier Space:
(Frequency)

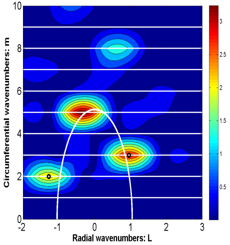

Front propagating outwards (radius increasing $R \in [2, 7]$, $\alpha \in [0, 2\pi]$)

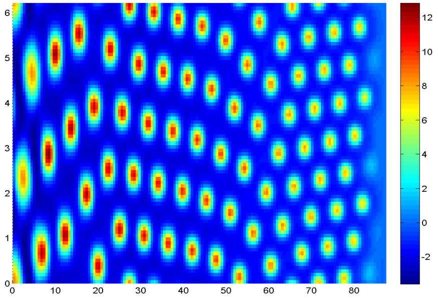

Fourier Space: (Frequency)

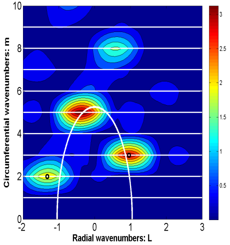

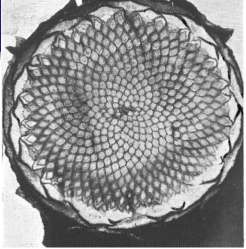

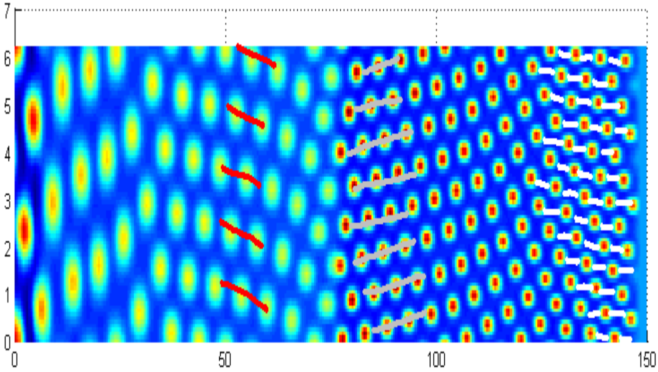
7
6
5
4
3
2
1
0
0
50
100
150

Outcome

Theorem: Under $R \to R\phi_{mn}$, $\phi_{mn} = \frac{m+n\phi}{m\phi+n} = \frac{1+\phi^2}{2\phi} \simeq \phi - 1/2$, the amplitude equations of two different Fibonacci sequences are isomorphic and in particular,

$E(1,2,3,5,8,...;R) = E(1,3,4,7,...;1.17R)$

1,3,4,7,...

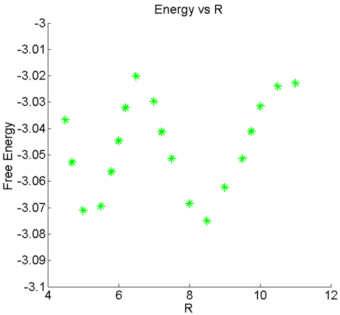

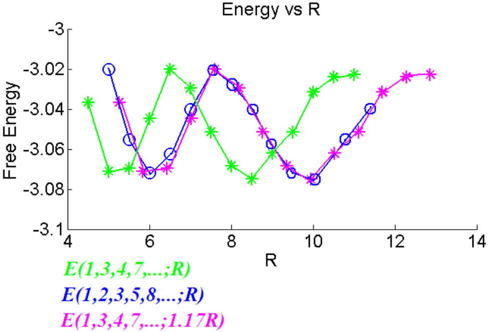

How are transitions achieved between whorls and Fibonacci sequences and between different Fibonacci sequences?

e.g. 2,2,4 → 2,3,5

e.g. 1,2,3,5, 8 → 1,3,4,7,..

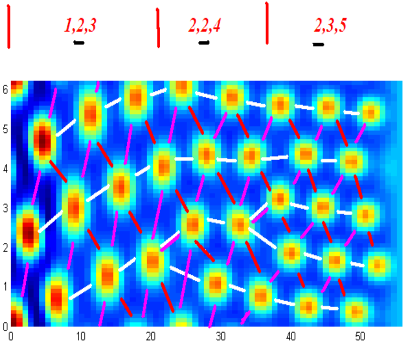

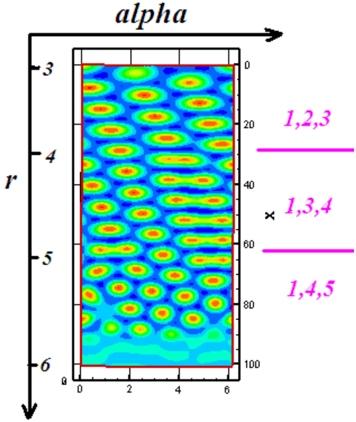

cf. Eckhaus, skew-varicose instabilities